Modeling the concentration-dependent permeation modes of the KcsA potassium ion channel

Peter Hugo Nelson*
Department of Physics, Benedictine University, Lisle, Illinois 60532, USA
(Received 16 February 2003; revised manuscript received 18 August 2003; published 18 December 2003)

The potassium channel from *Streptomyces lividans* (KcsA) is an integral membrane protein with sequence similarity to all known potassium channels, particularly in the selectivity filter region. A recently proposed model for ion channels containing either n or $(n-1)$ single-file ions in their selectivity filters [P. H. Nelson, J. Chem. Phys. **177**, 11396 (2002)] is applied to published KcsA channel K^+ permeation data that exhibit a high-affinity process at low concentrations and a low-affinity process at high concentrations [M. LeMasurier *et al.*, J. Gen. Physiol. **118**, 303 (2001)]. The kinetic model is shown to provide a reasonable first-order explanation for both the high- and low-concentration permeation modes observed experimentally. The low-concentration mode ($[K^+]<200$ mM) has a 200-mV dissociation constant of 56 mM and a conductance of 88 pS. The high-concentration mode ($[K^+]>200$ mM) has a 200-mV dissociation constant of 1100 mM and a conductance of 500 pS. Based on the permeation model, and x-ray analysis [J. H. Morais-Cabral *et al.*, Nature (London) **414**, 37 (2001)], it is suggested that the experimentally observed K^+ permeation modes correspond to an $n=3$ mechanism at high concentrations and an $n=2$ mechanism at low concentrations. The ratio of the electrical dissociation distances for the high- and low-concentration modes is 3:2, also consistent with the proposed $n=3$ and $n=2$ modes. Model predictions for K^+ channels that exhibit asymmetric current-voltage (I-V) curves are presented, and further validation of the kinetic model via molecular simulation and experiment is discussed. The qualitatively distinct I-V characteristics exhibited experimentally by Tl^+, NH_4^+, and Rb^+ ions at 100 mM concentration can also be explained using the model, but more extensive experimental tests are required for quantitative validation of the model predictions.

DOI: 10.1103/PhysRevE.68.061908 PACS number(s): 87.10.+e, 87.16.Uv, 87.16.Ac, 87.15.He

I. INTRODUCTION

Ion channels are proteins that conduct ions across the cell membrane. They represent the basic electrically conductive component of the nervous system and are the target of roughly a third of all drugs [1]. Recently, there has been much interest in the potassium-selective channel encoded by the kcsA gene from the bacteria *Streptomyces lividans* [2–4]. This channel is believed to be similar to other K^+ channels including voltage-dependent K^+ channels in vertebrates and invertebrates, Ca^{2+}-activated K^+ channels in vertebrates, K^+ channels from plants and bacteria, and cyclic nucleotide-gated cation channels [3]. High-resolution details of the KcsA potassium channel enzyme have shown that its active site is the selectivity filter—a narrow ion-attracting tube [3–5]. A relatively clear picture has emerged as to how ion channels function at a phenomenological level [4]. However, no simple quantitative model has been proposed for the complex variation of conductance with concentration observed experimentally under symmetrical salt conditions [6].

A major goal of ion channel biophysics is to understand the permeation behavior of ion channels based on their molecular structure [7–9]. The molecular dynamics (MD) simulation technique can directly investigate the microscopic details of permeation through ion channels of known structure. As a result, numerous MD simulations have been performed since the x-ray structure of KcsA was discovered, and valuable insights have been gained into the microscopic details of ion permeation [10–24]. A significant drawback of MD simulations is that they are presently limited to time scales comparable with that of permeation of a single ion ($\sim$10 ns), whereas electropermeation experiments typically measure currents on millisecond time scales. Thus, while investigation of a single conduction event is possible and free energies can be estimated, it is not currently possible to obtain statistically significant ion conduction data directly from MD simulation.

Brownian dynamics (BD) simulation methods simplify the computational problem by averaging out the rapid motion of water molecules and considering ionic transport as a stochastic process [25–31]. As a result, BD simulations can investigate substantially longer timescales than MD. These methods have qualitatively reproduced the saturating behavior of the KcsA channel conductance as a function of concentration (at high concentrations and at fixed voltage): however, BD simulations have generally predicted supralinear I-V curves (at constant concentration), in qualitative disagreement with experimental I-V curves (which are sublinear for K^+ permeation in KcsA for all concentrations investigated experimentally [6,32]). Neither of these molecular simulation methods have yet been able to simultaneously explain the K^+ conductance characteristics of the open KcsA ion channel as a function of both concentration and voltage.

Recently, a kinetic model was proposed for permeation in open single-file ion channels [33]. The kinetic model assumes that ionic transport can be modeled as a stochastic Markov process, in which all microscopic configurations of the channel are lumped into a small number of states associated with the ion occupancy of the channel selectivity filter. Transitions between states are modeled in a similar manner to traditional chemical kinetics. The states and the transition

*Fax: (253) 736-9389. Electronic address: pete@circle4.com

rates between them are intended to represent ensemble averages over all microscopic configurations and processes. In principle, the states and event rates can be determined from atomistic simulations [34]. MD and BD simulations have confirmed that the configuration space includes local minima corresponding to discrete ion occupancy states of the selectivity filter and that transitions between these states are relatively rapid, in qualitative agreement with the kinetic model. However, no analytic permeation model has yet been derived directly from molecular simulations.

In the recently proposed kinetic model [33], the lumped states were postulated based on the static x-ray structure of the KcsA ion channel selectivity filter [5]. A minimal kinetic model was then postulated based on the assumption that ion translocation within the channel selectivity filter is not rate limiting. The model has one kinetic parameter related to ion association and another related to dissociation from the selectivity filter. In addition, there is an electrical dissociation distance, representing the fraction of the transmembrane potential traversed by all mobile ions as an ion dissociates from an end of the selectivity filter (and enters the bulk aqueous phase). The formal mathematical structure of the kinetic model has recently been shown to be consistent with a number of microscopic K^+ permeation mechanisms in KcsA suggested by x-ray structural analysis and MD and BD simulations (performed at high K^+ concentrations). This comparison suggests that the kinetic model should be interpreted as an ensemble average over all possible permeation mechanisms [35].

A significant advantage of the kinetic model over atomistic computer simulations is that it provides a simple analytical expression for the average permeation rate as a function of the inner and outer solution concentrations and the transmembrane voltage. This analytical expression can be compared directly with single-channel permeation experiments. The model also provides a first-order explanation for the approximate Michaelis-Menten kinetics exhibited by many ion channels [1] and has been validated as a reasonable first-order approximation [33] for published Na^+ permeation data in gramicidin A [36] and for published K^+ ion permeation in the KcsA channel at relatively high concentrations [32].

LeMasurier *et al.* [6] recently investigated K^+ ion permeation in KcsA to lower concentrations than Meuser *et al.* [32]. From their experiments, LeMasurier *et al.* concluded that ''KcsA is a conventional K^+ channel. All ion permeation properties common to eukaryotic K^+ channels are recapitulated in KcsA: conduction by K^+, Rb^+, NH_4^+, Tl^+…, and complex variation of conductance with concentration, as expected for multi-ion occupancy in the pore, etc. Accordingly, we can safely view KcsA as an excellent structural paradigm for ion interactions in eukaryotic K^+ channels.'' LeMasurier *et al.* [6] did not fit any permeation model to their current-voltage (I-V) data, and the curves through their experimental data points were reported to have ''no theoretical meaning.'' Regarding K^+ permeation, LeMasurier *et al.* observed that ''[a]s expected for multi-ion single-file channels, the conductance-concentration curve cannot be even crudely fit by a rectangular hyperbola.'' Thus, the results of LeMasurier *et al.* [6] appear to be inconsistent with the proposed kinetic model [33] (which predicts a rectangular hyperbola for the conductance-concentration curve). Morais-Cabral *et al.* [5] recently proposed a kinetic model to explain K^+ and Rb^+ permeation in KcsA. Their model had 12 adjustable parameters for K^+ permeation and was implemented as a Monte Carlo simulation, but was not compared quantitatively with experimental permeation data.

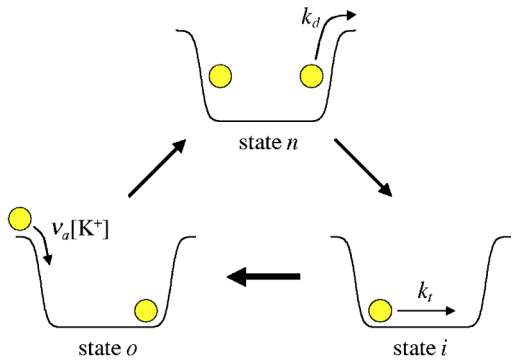

FIG. 1. Proposed double-occupancy ($n=2$) permeation mechanism for the selectivity filter of KcsA at low concentrations. Formally, the net flux has the same kinetics as the previously proposed triple-occupancy mechanism ($n=3$) (see text). All steps are reversible.

In this article, the apparent conflict between the experiments of LeMasurier *et al.* [6] and the recently proposed permeation model [33,35] is addressed. The model is introduced and its Michaelis-Menten predictions are summarized. An Eadie-Hofstee plot is used to show that K^+-ion permeation (at 200 mV) can be divided into two separate Michaelis-Menten permeation modes: one above 200 mM and one below 200 mM. Each of these modes is then shown to have a voltage dependency consistent with the model's predictions. A physical interpretation of this behavior is then suggested, based on the properties of the model and the x-ray structure of KcsA [3,5].

II. PERMEATION MODEL

Within the permeation model, the selectivity filter of the ion channel is modeled as an ion-attracting tube capable of containing either n or $(n-1)$ single-file ions (Fig. 1). For symmetric bathing solutions ($[K^+]_i=[K^+]_o=[K^+]$), the probability that the channel is occupied by n ions is given by the Hill-Langmuir equation

$$\theta_n=\frac{c^*}{1+c^*}, \tag{1}$$

where

$$c^*=[K^+]/K_M \tag{2}$$

is a concentration ''reduced'' [37] by a voltage-dependent Michaelis-Menten coefficient

$$K_M=(e^{\phi}+e^{-\phi})k_d/\nu_a=K_d\cosh\phi. \tag{3}$$

$\phi = ze_o \delta V/kT$, where δ is the sum of the electrical distances traveled by all n ions (each having charge ze_o) as the nth ion dissociates in the presence of a transmembrane voltage V at temperature T (k is the Boltzmann constant) [35]. k_d is the dissociation rate constant, and ν_a is the association rate constant. $K_d = 2k_d/\nu_a$ is a (zero-voltage) equilibrium dissociation constant. The net permeation rate J is given by

$$J = k_{\max}\theta_n, \tag{4}$$

where $k_{\max}$ is the maximum net transfer rate of ions at voltage V, which is given by

$$k_{\max} = \frac{e^{\phi} - e^{-\phi}e^{-\omega}}{1 + e^{-\omega}} k_d, \tag{5}$$

where $\omega = ze_o \ell V/kT$ and $\ell = 1 - 2\delta$. The experimentally measured permeation rate J can be divided by $k_{\max}$, to provide a reduced permeation rate

$$j^* = \frac{c^*}{1 + c^*}. \tag{6}$$

Thus, within the model, j^* is a universal Michaelis-Menten function of c^*, wherein the reduced permeation rate j^* is equal to the time-average occupancy state θ_n of the open channel [33].

III. COMPARISON WITH EXPERIMENT

LeMasurier *et al.* [6] found that KcsA generally exhibited asymmetrical I-V characteristics. As discussed in the Appendix, the permeation model can be modified in a straightforward manner to account for asymmetric I-V curves. However, because the raw electropermeation data exhibited excessive signal noise at negative potentials (which was attributed to rapid unresolved fluctuations of the channel), LeMasurier *et al.* confined their analysis to I-V data at positive voltages. The proposed kinetic model relates to steady-state (nonfluctuating) current of the open channel. Hence, following the approach of LeMasurier *et al.*, only positive voltage I-V data will be compared with the permeation model.

LeMasurier *et al.* [6] reported KcsA K^+ permeation data (at 200 mV) from low concentrations ($[K^+] = 5$ mM) though high concentrations ($[K^+] = 1600$ mM). They identified two K^+ ion conduction modes: a quickly saturating low-concentration mode and a slowly saturating high-concentration mode. These data are compared with the Michaelis-Menten predictions of the model by making an Eadie-Hofstee plot of the experimental data as shown in Fig. 2, using

$$g = g_{\max} - K_M\left(\frac{g}{[S]}\right), \tag{7}$$

where the conductance is given by $g = ze_o J/V$, and the maximum conductance is given by $g_{\max} = ze_o k_{\max}/V$. Thus, if a channel exhibits Michaelis-Menten kinetics (at fixed voltage) as predicted by the kinetic model, then a plot of g versus $(g/[S])$ will yield a straight line with intercept $g_{\max}$ and slope $-K_M$. The data reported by LeMasurier *et al.* [6] exhibit two Michaelis-Menten permeation modes as suggested by the fitted model (straight lines). At low concentrations, $[K^+] < 200$ mM, there is a high-affinity $K_M(200\text{ mV}) = 56$ mM, low-conductance $g_{\max}(200\text{ mV}) = 88$ pS permeation mode. At high concentrations, $[K^+] > 200$ mM, there is a low-affinity $K_M(200\text{ mV}) = 1100$ mM, high-conductance $g_{\max}(200\text{ mV}) = 500$ pS permeation mode.

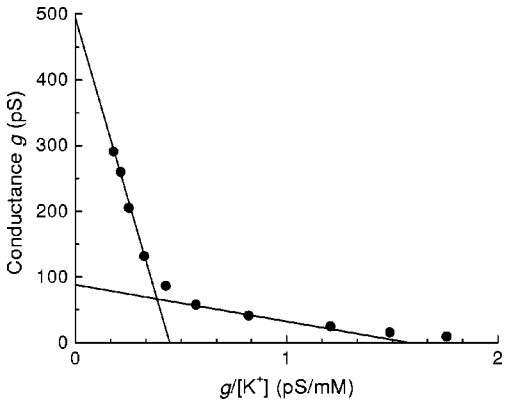

FIG. 2. Examining the saturating behavior of K^+ ion permeation in KcsA under symmetric solution conditions using an Eadie-Hofstee plot [Eq. (7)]. Symbols-experimental data for an applied transmembrane voltage of +200 mV are reproduced (with permission) from LeMasurier *et al.* [6]. The straight lines represent nonlinear least-squares fits to the proposed model (Table I), using all the available experimental current-voltage (I-V) data in two concentration ranges: high concentrations ($[K^+] > 200$ mM (see Fig. 3)), and low concentrations ($[K^+] < 200$ mM (see Fig. 4)).

Figures 3 and 4 show the fit of model to the high and low $[K^+]$ permeation data of LeMasurier *et al.*, [6] respectively. The fitted parameters k_d, ν_a, and δ (Table I) were obtained by least-squares fits to the open-channel current data using all available data above and below 200 mM. For comparison, the previously reported parameters [33] for KcsA permeation in a different bilayer and between symmetric pH solutions [32] are also listed. In addition to the kinetic parameters, the equilibrium dissociation constant $K_d = 2k_d/\nu_a$ is also tabulated. This quantity represents the binding affinity of the channel for the nth ion at zero volts.

The data for a single I-V curve in Figs. 3(A) and 4(A) are spread out in Figs. 3(B) and 4(B) by the voltage dependences of $k_{\max}$ and K_M. For each I-V curve, the high-voltage currents correspond to the lowest values in the j^*-c^* plots, and the low-voltage currents correspond to the highest values in the j^*-c^* plots. The large (and apparently systematic) deviations seen at high c^* values [in Figs. 3(B) and 4(B)] result from this nonlinear transformation. As can be seen in Figs. 3(A) and 4(A), the experimental deviations at 25 mV (between the raw experimental current data and the fitted model) are comparable in magnitude with the deviations for the remainder of the experimental data points.

The least-squares fit to the low-concentration data is biased to fit the $[K^+] = 20$, 50, and 100 mM experiments because there are eight experimental data points for each of these concentrations (Fig. 4), whereas for $[K^+] = 5$ and

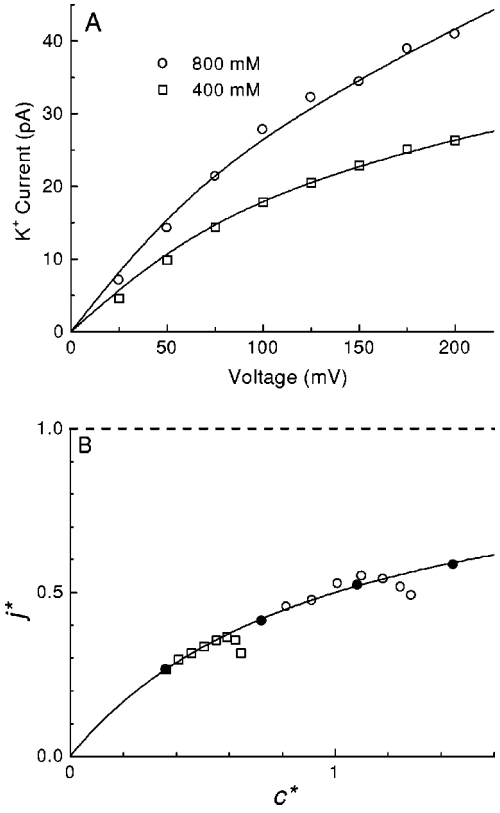

FIG. 3. Comparing the proposed permeation model (solid lines) with high-concentration ($[K^+]>200$ mM) experimental data. The experimental data points are reproduced (with permission) from LeMasurier *et al.* [6]. (A) Model current-voltage (I-V) curves (solid lines) for K^+-ion permeation between symmetric $[K^+]$ solutions with $[K^+]=400$ and 800 mM. Fitted parameters—see Table I. (B) Corresponding occupancy-states plot of the reduced permeation rate j^* vs reduced concentration c^*. Open symbols—data from Fig. 3(A). Solid symbols—data from Fig. 2.

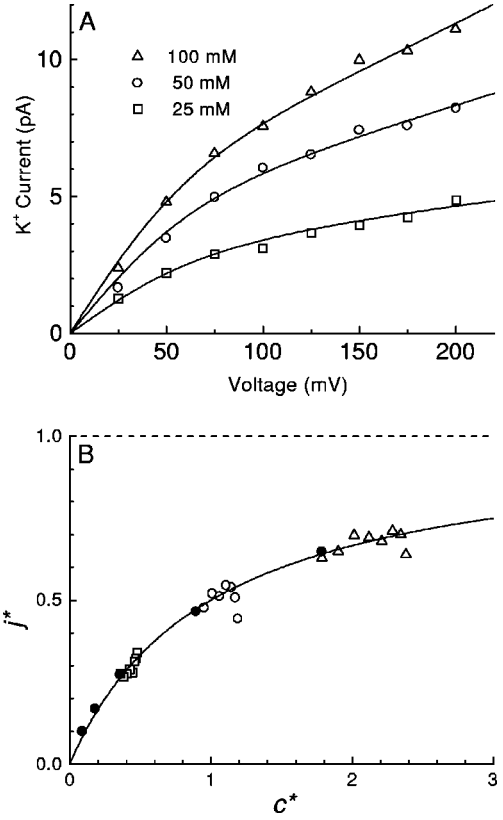

FIG. 4. Comparing the proposed permeation model (solid lines) with experimental data at low concentrations ($[K^+]<200$ mM). Symbols—experimental data reproduced (with permission) from LeMasurier *et al.* [6]. (A) Current-voltage (I-V) plot for K^+ ion permeation between symmetric $[K^+]$ solutions with $[K^+]=20$, 50, and 100 mM. Fitted parameters—see Table I. (B) Corresponding occupancy-states plot of the reduced permeation rate j^* vs reduced concentration c^*. Open symbols—data from Fig. 4(A). Solid symbols—data from Fig. 2.

10 mM only a single experimental data point (at 200 mV) was reported. It would be desirable to include a similar number of data points for these lowest concentrations (highest values of $g/[K^+]$ in Fig. 2) so that the slope $-K_M(200\text{ mV})$ and intercept $g_{\max}(200\text{ mV})$ of the low-concentration line in Fig. 2 can be estimated more accurately.

Figure 5 shows the preliminary fit of the model to the other ions (Tl^+, NH_4^+, and Rb^+) using a single permeation mode for the experimental data at concentrations less than 200 mM. Due to the relatively small amount of available experimental data, the model parameters in Table I should be considered as preliminary estimates. I-V curves covering a range of concentrations are required to further test the model predictions.

IV. DISCUSSION

A. K^+ ion permeation

LeMasurier *et al.* [6] identified the low-concentration mode with ions entering two high-affinity sites in the KcsA pore, one in the aqueous central cavity of the pore (outside of the selectivity filter) and another high-affinity site inside the selectivity filter. The high-concentration mode was identified with the gradual filling of a low-affinity site in the selectivity filter. In contrast, the present model considers the central cavity to be an extension of the bulk intracellular aqueous solution, and hence, only ion binding within the selectivity filter is explicitly considered. This approximation is consistent with the recently discovered open pore conformation of potassium channels, which shows that the central cavity is essentially continuous with the inner solution and that the cavity is at the same membrane potential as the internal solution (under equilibrium conditions) [38].

The permeation model proposed by Morais-Cabral *et al.* [5] provides for an arbitrary concurrent combination of one-, two-, and three-ion permeation modes, with all three ions being located in the selectivity filter. This model is thus conceptually similar to traditional site-based models of single-file permeation, which provide for all possible occupancies of the channel [1,39]. The present model provides a significant simplification to this traditional approach as only states containing n or $(n-1)$ single-file ions are considered, consistent with the approach previously proposed by Schumaker and Mackinnon [40,41].

TABLE I. KcsA permeation parameters obtained from data reported by LeMasurier *et al.* [6].

Ion (S)	$[S]^a$	k_d (s^{-1})	ν_a ($s^{-1} M^{-1}$)	K_d (mM)	δ
K^+ [b]	high	1.9×10^8	6.1×10^8	630	0.18
K^+	high	1.9×10^8	6.1×10^8	610	0.15
K^+	low	5.0×10^7	2.4×10^9	42	0.10
Tl^+ [c]	low	2×10^7	2×10^9	30	0.01
NH_4^+ [c]	low	1×10^7	1×10^9	20	0.2
Rb^+ [c]	low	3×10^6	3×10^9	2	0.3

[a]High, $[S]>200$ mM, and low, $[S]<200$ mM.
[b]Previous fit [33] to data reported by Meuser *et al.* [32].
[c]Parameters are preliminary estimates—more experimental data are required.

Based on x-ray analysis [5], the high-concentration permeation mode reported by Meuser *et al.* [32] was interpreted as a KcsA selectivity filter with $n=3$ partially dehydrated K^+ ions in the conductive state of the selectivity filter [33]. Similar model parameters have been obtained (Table I) for the low-affinity high-conductance ($[K^+]>200$ mM) permeation mode observed by LeMasurier *et al.*, [6] suggesting that they observed the same permeation mode as observed by Meuser *et al.* [32] (also for $[K^+]>200$ mM).

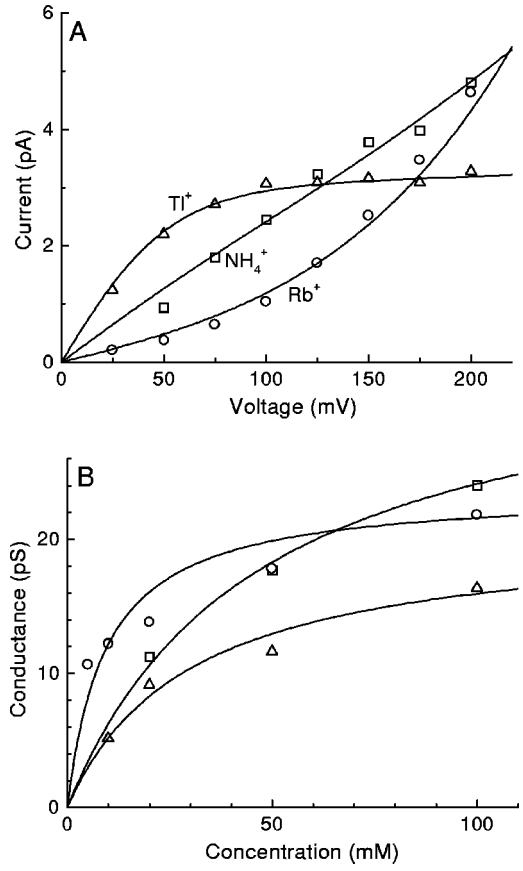

FIG. 5. Preliminary comparison of the proposed permeation model (solid lines) with experiment at low substrate ion concentrations ($[S]<200$ mM). The experimental data points are reproduced (with permission) from LeMasurier *et al.* [6]. (A) Current-voltage (I-V) plots for ion permeation between symmetric $[S]=100$ mM solutions. Fitted parameters—see Table I. (B) Conductance-concentration plots (at 200 mV).

The complex variation of conductance with concentration reported by LeMasurier *et al.* [6] has been resolved into two distinct Michaelis-Menten permeation modes (Figs. 2–4). The dissociation rate constant k_d for the low-concentration mode is nearly 4 times smaller and the association rate constant ν_a is nearly 4 times larger than the corresponding high-concentration values. The resulting equilibrium dissociation constant K_d is nearly 15 times smaller than the high-concentration value. A potential explanation for this bimodal behavior is that the number of ions in the conductive state of the channel changes with concentration. From their x-ray analysis, Morais-Cabral *et al.* [5] inferred that the KcsA selectivity filter normally contains a single K^+ ion at low concentrations. Based on this observation, it is suggested that K^+ conduction at low concentrations $[K^+]<c_t$ might proceed according to an $n=2$ permeation mechanism (see Fig. 1).

The hypothesis that the low-concentration mode has two ions in the conductive state is further supported by the 2:3 ratio of the electrical dissociation distances for the low and high modes, respectively. As discussed recently [35], the electrical dissociation distance is the sum of the electrical dissociation distances ε for each ion. If it is assumed that ε ($=0.05$) is the same for each mode (and all n ions), then the electrical dissociation distance for the $n=2$ mode is $\delta=2\varepsilon$, and the $n=3$ mode has $\delta=3\varepsilon$, consistent with the experimental values of 0.10 and 0.15, respectively.

The concentration c_t that separates the two modes is expected to be both voltage and temperature dependent (independent of any protein relaxation at low temperatures). From low-temperature x-ray analysis at zero volts $c_t<20$ mM [5], whereas at $V=200$ mV and room temperature $c_t\approx200$ mM (Fig. 2). Experimental investigation of the temperature dependence of c_t (and the other permeation parameters) can be made by performing additional permeation experiments, or x-ray experiments, at different voltages and/or temperatures.

It is further suggested that the transition in permeation mechanism at $[K^+]\approx c_t$ might be caused by a relatively rapid change in the number of single-file water molecules trapped between the two ions in a doubly occupied KcsA selectivity filter (as the concentration is varied). At high concentrations, a single water molecule is thought to separate the ions in the *nonconductive* doubly occupied state [5]. This is consistent with the proposed triple-occupancy permeation mechanism at high K^+ concentrations [33]. At low concentrations, there may be two (or more) water molecules trapped between the ions in the *conductive* doubly occupied state of the selectivity filter (state *n* in Fig. 1). The implied transition from singly occupied to doubly occupied *nonconductive* selectivity filter states appears to be qualitatively consistent with the x-ray data of Morais-Cabral *et al.* [5]. The experimentally observed permeability change is thus interpreted as a form of concentration-dependent ''mode switching'' caused by a transition in the possible occupancy state(s) of the channel's selectivity filter. Changes in the selectivity filter have previously been proposed as a cause of channel gating

[4,42,43]. The number of water molecules in the selectivity filter can be investigated experimentally by streaming potential experiments [1].

The proposed high-concentration mode thus corresponds to a cycle around the *B-C-A* states identified by Morais-Cabral *et al.*, [5] and the low-concentration mode corresponds to either the *D-E-F* or the *G-H-F* cycle or a combination of both. The difference between the later two cycles is that the former provides for (single ion)–(water molecule) exchanges, while the later provides for concerted association and dissociation. The constant ε explanation for the 2:3 ratio of the electrical dissociation distances, requires a concerted association and dissociation mechanism (wherein all ions move the same electrical distance $\varepsilon = 0.05$ in both modes). However, (single ion)–(water molecule) mechanisms would imply that the nth ion travels a shorter electrical distance in the $n=2$ mode. Notwithstanding this distinction, both of these mechanisms (or combinations of both) may be represented by the present kinetic model [35].

An alternate explanation for the experimentally observed mode switching is a concentration-dependent change in the ion binding characteristics of the selectivity filter. This might be caused by a protein conformation change or by ion binding outside of the selectivity filter. Thus, the change in permeation mode may not be accompanied by a change in the number of ions (n) in the conductive state(s) of the channel. According to the kinetic model, n cannot be probed by experiments within the copermeation eigenmode, but tracer counterpermeation (or mixed permeation mode) experiments should be able to test the n-dependent predictions of the model [33].

In principle, molecular simulations should be able to test these hypotheses. As has already been shown, the kinetic model appears to be consistent with a number of distinct $n=3$ permeation mechanisms suggested by atomistic simulations at high concentrations [35]. Molecular simulations should also be able to investigate the permeation mechanism(s) that operate at low concentrations and the transition between the experimentally observed high- and low-concentration modes. In addition to qualitative comparison, it would be desirable to investigate whether any quantitative relationship can be established between molecular simulation and the kinetic model. The kinetic model makes simple predictions (viz., K_d) for how the (zero-volt) equilibrium occupancy of the channel selectivity filter changes with concentration. In addition, the kinetic model makes specific predictions (viz., K_M) for how the steady-state occupancy varies in the presence of a nonzero transmembrane voltage. These steady-state occupancies might be investigated using molecular simulation techniques [34] and compared with the predictions of the kinetic model and experiment. A potentially more difficult task will be to investigate the whether any correspondence can be established between the kinetic model parameters and molecular simulations. Of particular interest is the electrical dissociation distance δ, which governs voltage dependence within the model.

The kinetic model makes specific predictions for how the shapes of the *I-V* curves change with concentration for both symmetric and asymmetric bathing solutions. The Appendix sets out the model predictions for a channel selectivity filter having symmetric ion binding characteristics but asymmetric *I-V* curves. Since it is believed that the ion conduction pore is conserved among K^+ channels [44], this generalized kinetic model may find applicability to K^+ channels other than KcsA.

B. Permeation of other ions

LeMasurier *et al.* [6] found that permeation of other ions in KcsA exhibit qualitatively different experimental *I-V* characteristics from K^+ and from each other. These appear to be consistent with the proposed model [Fig. 5(A)]. At a concentration of 100 m*M*: Tl^+ exhibits an essentially voltage-independent permeation rate above 100 mV, suggesting that the association step is rate limiting; Rb^+ exhibits a supralinear voltage dependence, suggesting that the dissociation step is rate limiting; and NH_4^+ exhibits an approximately Ohmic *I-V* dependence over the experimental voltage range, suggesting intermediate behavior [33]. Because there is insufficient experimental data for the other ions (Tl^+, NH_4^+, and Rb^+), the model parameters in Table I should be considered to be preliminary estimates. Additional experiments might be used to test for the concentration-dependent changes in *I-V* behavior predicted by the model [33].

The three distinct qualitative *I-V* behaviors shown in Fig. 5(A) represent the full range of behavior possible within the permeation model at low voltages (<200 mV). Within the model, the shape of an *I-V* curve is determined by two parameters, the electrical dissociation distance δ, and the zero-voltage reduced concentration $c_o^* = [K^+]/K_d$. For small values of δ (less than about 0.15), *I-V* curves at all concentrations c_o^* are sublinear, leveling off more rapidly for smaller values of δ. For larger values of δ (greater than about 0.15), the curves are able to become supralinear, with the possible *I-V* behaviors depending upon both parameters. At low values of c_o^* (e.g., $c_o^* < 2.4$ for $\delta = 0.25$), the *I-V* curves are sublinear, and for high values of c_o^* (e.g., $c_o^* > 2.4$ for $\delta = 0.25$), the *I-V* curves are supralinear. At intermediate values of c_o^* (e.g., $c_o^* \cong 2.4$ for $\delta = 0.25$), the *I-V* curves are approximately linear for low voltages ($V < 200$ mV).

Due to the corresponding occupancy states property of the kinetic model [33], conductance-concentration plots are always expected to exhibit Michaelis-Menten saturating behavior at any fixed voltage (for a single permeation mode), thus providing a simple test of the model's potential applicability. However, measurement of entire *I-V* curves (over as wide a range of concentration as possible) is required to test the voltage-dependent predictions of the model and to determine the model parameters more accurately.

LeMasurier *et al.* [6] also performed an asymmetric $[K^+]$ solution (100 m*M* internal/20 m*M* external) permeation experiment, which appears to be qualitatively consistent with the predictions of the proposed model [33]. The difference (~10 mV) between the experimental reversal potential and the that predicted by the Nernst equation was identified by LeMasurier *et al.* to be an experimental uncertainty. This ex-

perimental uncertainty precludes quantitative comparison with the model predictions.

C. Conclusion

Each of the high- and low-concentration KcsA permeation modes identified by LeMasurier *et al.* [6] have been shown to be consistent with the scaling predictions of the recently proposed single-file permeation model [33]. At low concentrations, there is a high-affinity low-conductance K^+ ion permeation mode, and at high concentrations, there is a low-affinity high-conductance permeation mode. At room temperature these two Michaelis-Menten modes are separated by a transition concentration of $c_t \approx 200$ mM (at $V = 200$ mV). Preliminary analysis of the permeation of other ions (Tl^+, NH_4^+, and Rb^+) has been found to be consistent with the proposed model, but additional experiments are required to test the model's quantitative predictions.

Based on the properties of the permeation model and x-ray analysis of Morais-Cabral *et al.* [5], it has been suggested that the experimentally observed K^+ permeation modes correspond to a triple-occupancy ($n=3$) mechanism at high concentrations and a double-occupancy ($n=2$) mechanism at low concentrations, with two and one water molecules separating the ions in the double- and triple-occupancy mechanisms, respectively. The experimental ratio of 2:3 for the electrical dissociation distances in the $n=2$ and $n=3$ modes is consistent with association and dissociation occurring via a concerted mechanism, wherein all n ions move a similar electrical distance in each permeation mode. Molecular simulations should be able to test these hypotheses.

Further experimental validation of the model will require investigation of the temperature and voltage dependence of the transition concentration c_t via x-ray and/or permeation experiments. Tracer counterpermeation and/or asymmetric-solution experiments, preferably with well-defined open-channel currents at negative potentials, can be used to validate predictions of the model that have not yet been tested.

ACKNOWLEDGMENTS

The author wishes to thank LeMasurier *et al.* [6] for making their experimental data publicly available at the J. Gen. Physiol. web site (http://www.jgp.org/cgi/content/full/118/3/303/DC1/1). Dr. Stefan Winkler is thanked for helpful comments on an earlier version of the manuscript. Support from the NIH (Grant No. GM20584) and from the HHMI (Grant No. 52002669) is gratefully acknowledged.

APPENDIX: ASYMMETRIC CHANNELS

The primary aim of the present article is to address the apparent conflict between the LeMasurier *et al.* [6] experiments and the proposed kinetic model. Because LeMasurier *et al.* did not consider their negative voltage permeation data to be representative of steady-state open-channel current, these data are not analyzed in this article. However, since the kinetic model may be applicable to other K^+ channels (which exhibit asymmetric open channel I-V curves), this appendix sets out a simple generalization of the theory, showing how channel asymmetry outside of the central ℓ region of the selectivity filter affects open-channel current.

In the simplified model, it is assumed that the ion binding ℓ region of the selectivity filter is symmetric and that the i and o states of the channel are equally probable at zero volts. This symmetry is reflected in the ionic potential profile (Fig. 1), which, in turn, is supported by the symmetric K^+ ion density observed in the x-ray structure at 20 and 200 mM KCl [5]. A simple form of channel asymmetry can be introduced into the model by replacing δ with δ_i and δ_o at the inner and outer ends of the selectivity filter respectively and/or by making the association-dissociation rate constants end dependent [i.e., by replacing (k_d and ν_a) with (k_i and ν_i) and (k_o and ν_o) at the inner and outer ends of the selectivity filter, respectively]. However, in order to retain the static K^+-ion symmetry observed in the x-ray structure of the KcsA selectivity filter [5], the zero-volt equilibrium dissociation constant K_d must be the same at both ends of the selectivity filter, i.e.,

$$\frac{k_i}{\nu_i} = \frac{k_o}{\nu_o} = \frac{K_d}{2}. \tag{A1}$$

Because the binding affinity at zero volts does not depend on the electrical dissociation distances, there is no constraint on placed on δ_i and δ_o by the static x-ray structure.

For a single permeation mode of an asymmetric channel exposed to asymmetric solutions of a substrate ion S (i.e., $[S]_i \neq [S]_o$), the channel occupancy is once again given by Eq. (1), the net flux is given by Eq. (4), and the reduced flux is given by Eq. (6). However, the reduced concentration is now given by

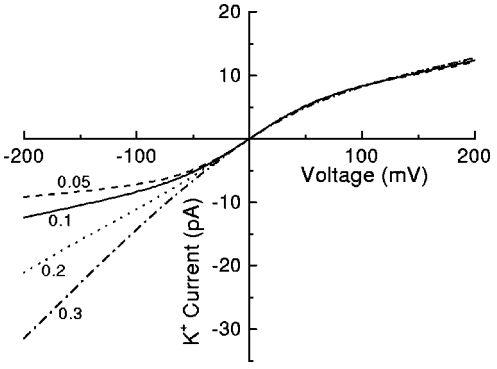

FIG. 6. Theoretical rectification produced by an asymmetric ion channel: effect of varying the inner electrical dissociation distance δ_i (figure parameter) on the open-single-channel I-V curve, while holding the outer electrical dissociation distance δ_o (=0.1) constant. For simplicity, the concentrations and association and dissociation rate constants were assumed to be symmetrical (i.e., $[K^+]_i = [K^+]_o = 150$ mM, $\nu_i = \nu_o = \nu_a = 6.1\times10^8$ s^{-1} M^{-1}, and $k_i = k_o = k_d = 5.0\times10^7$ s^{-1}—see the Appendix).

$$c^* = \frac{[S]_i + \frac{k_o}{k_i} e^{-\omega} [S]_o}{(1+e^{-\omega}) K_d \left(\frac{k_o}{k_i} e^{\phi_o} + e^{-\phi_i} \right) \Big/ 2}, \qquad \text{(A2)}$$

where $k_o/k_i = \nu_o/\nu_i$ from Eq. (A1) and the maximum net transfer rate of ions is given by

$$k_{\max} = \frac{e^{\phi_o}[S]_i - e^{-\phi_i} e^{-\omega}[S]_o}{[S]_i + \frac{k_o}{k_i} e^{-\omega}[S]_o} k_o, \qquad \text{(A3)}$$

where $\phi_i = z e_o \delta_i V/kT$, $\phi_o = z e_o \delta_o V/kT$, $\omega = z e_o \ell V/kT$, and $\ell = 1 - \delta_i - \delta_o$.

As shown in Fig. 6, changing just the inner electrical dissociation distance δ_i can have a marked effect on the negative voltage current, while having a minimal effect on the positive voltage current. For smaller values of δ_i (relative to δ_o), the open channel is outwardly rectifying in qualitative agreement with the measurements of LeMasurier *et al.* [6] for the KcsA K^+ channel. When $\delta_i = \delta_o$, the open channel current is symmetrical consistent with the data reported by Meuser *et al.* [32] for the KcsA K^+ channel. Heginbotham *et al.* [45] found (under similar permeation conditions to LeMasurier *et al.* [6]) that Y82C substitution preserved the basic KcsA properties but also resulted in nearly symmetrical *I-V* characteristics. For larger values of δ_i, the open channel is inwardly rectifying in qualitative agreement with the measurements of Jiang *et al.* [46] for the MthK channel, a K^+ channel which has a similar selectivity filter to KcsA [38].

Further validation of the model predictions will require measurement of open-channel *I-V* curves for both negative and positive voltages over a wide range of concentrations. A relatively wide range of concentrations is required to investigate the various limiting cases predicted by the model [33].

[1] B. Hille, *Ion Channels of Excitable Membranes*, 3rd ed. (Sinauer Associates, Sunderland, MA, 2001).
[2] H. Schrempf *et al.*, EMBO J. **14**, 5170 (1995).
[3] D. A. Doyle *et al.*, Science **280**, 69 (1998).
[4] G. Yellen, Nature (London) **419**, 35 (2002).
[5] J. H. Morais-Cabral, Y. Zhou, and R. MacKinnon, Nature (London) **414**, 37 (2001).
[6] M. LeMasurier, L. Heginbotham, and C. Miller, J. Gen. Physiol. **118**, 303 (2001).
[7] S. Kuyucak, O. S. Andersen, and S. H. Chung, Rep. Prog. Phys. **64**, 1427 (2001).
[8] D. P. Tieleman *et al.*, Q. Rev. Biophys. **34**, 473 (2001).
[9] S. H. Chung and S. Kuyucak, Eur. Biophys. J. **31**, 283 (2002).
[10] T. W. Allen, S. Kuyucak, and S. H. Chung, Biophys. J. **77**, 2502 (1999).
[11] L. Guidoni, V. Torre, and P. Carloni, Biochemistry **38**, 8599 (1999).
[12] T. W. Allen *et al.*, J. Chem. Phys. **112**, 8191 (2000).
[13] J. Åqvist and V. Luzhkov, Nature (London) **404**, 881 (2000).
[14] S. Bernèche and B. Roux, Biophys. J. **78**, 2900 (2000).
[15] C. E. Capener *et al.*, Biophys. J. **78**, 2929 (2000).
[16] L. Guidoni, V. Torre, and P. Carloni, FEBS Lett. **477**, 37 (2000).
[17] V. B. Luzhkov and J. Åqvist, Biochim. Biophys. Acta **1481**, 360 (2000).
[18] M. S. Sansom *et al.*, Trends Biochem. Sci. **25**, 368 (2000).
[19] I. H. Shrivastava and M. S. Sansom, Biophys. J. **78**, 557 (2000).
[20] S. Bernèche and B. Roux, Nature (London) **414**, 73 (2001).
[21] P. C. Biggin *et al.*, Biochim. Biophys. Acta **1510**, 1 (2001).
[22] V. B. Luzhkov and J. Åqvist, Biochim. Biophys. Acta **1548**, 194 (2001).
[23] C. E. Capener and M. S. Sansom, J. Phys. Chem. B **106**, 4543 (2002).
[24] I. H. Shrivastava *et al.*, Biophys. J. **83**, 633 (2002).
[25] S. H. Chung *et al.*, Biophys. J. **77**, 2517 (1999).
[26] S. H. Chung and S. Kuyucak, Clin. Exp. Pharmacol. Physiol. **28**, 89 (2001).
[27] R. J. Mashl *et al.*, Biophys. J. **81**, 2473 (2001).
[28] A. Burykin *et al.*, Proteins **47**, 265 (2002).
[29] S. H. Chung, T. W. Allen, and S. Kuyucak, Biophys. J. **83**, 263 (2002).
[30] S. H. Chung, T. W. Allen, and S. Kuyucak, Biophys. J. **82**, 628 (2002).
[31] S. Bernèche and B. Roux, Proc. Natl. Acad. Sci. U.S.A. **100**, 8644 (2003).
[32] D. Meuser *et al.*, FEBS Lett. **462**, 447 (1999).
[33] P. H. Nelson, J. Chem. Phys. **117**, 11 396 (2002).
[34] D. Frenkel and B. Smit, *Understanding Molecular Simulation—From Algorithms to Applications*, 2nd ed. (Academic Press, San Diego, 2002).
[35] P. H. Nelson, J. Chem. Phys. **119**, 6981 (2003).
[36] D. D. Busath *et al.*, Biophys. J. **75**, 2830 (1998).
[37] D. A. MacQuarrie, *Statistical Mechanics* (University Science Books, Sausalito, CA, 2000).
[38] Y. Jiang *et al.*, Nature (London) **417**, 523 (2002).
[39] B. Hille and W. Schwarz, J. Gen. Physiol. **72**, 409 (1978).
[40] M. F. Schumaker and R. MacKinnon, Biophys. J. **58**, 975 (1990).
[41] M. F. Schumaker, Biophys. J. **63**, 1032 (1992).
[42] L. Kiss and S. J. Korn, Biophys. J. **74**, 1840 (1998).
[43] Y. Zhou *et al.*, Nature (London) **414**, 43 (2001).
[44] Z. Lu, A. M. Klem, and Y. Ramu, Nature (London) **413**, 809 (2001).
[45] L. Heginbotham *et al.*, J. Gen. Physiol. **114**, 551 (1999).
[46] Y. Jiang *et al.*, Nature (London) **417**, 515 (2002).